Earth and Planetary Science Letters 422 (2015) 75–86

Contents lists available at ScienceDirect

Earth and Planetary Science Letters

www.elsevier.com/locate/epsl

Recording the transition from flare-up to steady-state arc magmatism at the Purico–Chascon volcanic complex, northern Chile

Dale H. Burns [a,*,1], Shanaka L. de Silva [a], Frank Tepley III [a], Axel K. Schmitt [b], Matthew W. Loewen [a]

[a] College of Earth, Ocean, and Atmospheric Sciences, Oregon State University, Corvallis, OR 97731, USA
[b] Department of Earth, Planetary, and Space Sciences, University of California at Los Angeles, Los Angeles, CA 90095, USA

ARTICLE INFO

Article history:
Received 6 December 2014
Received in revised form 31 March 2015
Accepted 1 April 2015
Available online 22 April 2015
Editor: T. Mather

Keywords:
Central Andes
continental arc evolution
ignimbrite flare-up
steady-state arc
in situ Sr isotopes
crystal isotope stratigraphy

ABSTRACT

The long-term evolution of continental magmatic arcs is episodic, where a few transient events of high magmatic flux or flare-ups punctuate the low-flux magmatism or "steady state" that makes up most of the arc history. How this duality manifests in terms of differences in crustal architecture, magma dynamics and chemistry, and the time scale over which transitions occur is poorly known. Herein we use multiscale geochemical and isotopic characteristics coupled with geothermobarometry at the Purico–Chascon Volcanic Complex (PCVC) in the Central Andes to identify a transition from flare-up to steady state arc magmatism over ∼800 kyr during which significant changes in upper crustal magmatic dynamics are recorded.

The PCVC is one of the youngest volcanic centers related to a 10–1 Ma ignimbrite flare-up in the Altiplano–Puna Volcanic Complex of the Central Andes. Activity at the PCVC initiated 0.98 ± 0.03 Ma with the eruption of a large 80–100 km^3 crystal-rich dacite ignimbrite. High, restricted $^{87}Sr/^{86}Sr$ isotope ratios between 0.7085 and 0.7090 in the bulk rock and plagioclase crystals from the Purico ignimbrite, combined with mineral chemistry and phase relationships indicate the dacite magma accumulated and evolved at relatively low temperatures around 800–850 °C in the upper crust at 4–8 km depth. Minor andesite pumice erupted late in the ignimbrite sequence records a second higher temperature (965 °C), higher pressure environment (17–20 km), but with similar restricted radiogenic bulk rock $^{87}Sr/^{86}Sr$ = 0.7089–0.7091 to the dacites. The compositional and isotopic characteristics of the Purico ignimbrite implicate an extensive zone of upper crustal mixing, assimilation, storage and homogenization (MASH) between ∼30 and 4 km beneath the PCVC ∼1 Ma.

The final eruptions at the PCVC $<0.18 \pm 0.02$ Ma suggest a change in the magmatic architecture beneath the PCVC. These eruptions produced three small <6 km^3 crystal-rich dacite lava domes with radiogenic bulk rock $^{87}Sr/^{86}Sr$ ratios ranging from 0.7075 to 0.7081, that contain abundant basaltic-andesite inclusions with relatively low bulk rock $^{87}Sr/^{86}Sr$ ratios of 0.7057–0.7061. Plagioclase and amphibole in the host lava of Cerro Chascon, the largest of the domes, record two distinct magmatic environments; an upper crustal environment identical to that recorded in the Purico ignimbrite, and a second deeper, ∼15–20 km depth, higher temperature (∼922–1001 °C) environment. This deeper environment is recorded in textures and compositions of distinct mineral phases, and in intracrystalline isotope ratios. Plagioclase cores in the host dacite lava and mafic inclusions have *in situ* $^{87}Sr/^{86}Sr$ isotopic compositions of 0.7083 to 0.7095, broadly similar to plagioclase from the Purico ignimbrite. In contrast, plagioclase rims and microphenocrysts in the mafic inclusions are isotopically distinct with lower $^{87}Sr/^{86}Sr$ isotope ratios (0.7057 to 0.7065 and 0.7062 to 0.7064, respectively) that overlap with the regional isotopic "baseline" compositions that are parental to the modern arc lavas.

The textural and compositional characteristics of the PCVC attest to two distinct stages in its history. At ∼1 Ma the system was broadly homogeneous and dominantly dacitic recording extensive upper crustal magmatism. By ∼0.2 Ma the PCVC had transitioned to a more compositionally heterogeneous, smaller volume, mixed dacite to basaltic-andesite system, coinciding with the appearance of less-enriched "baseline" compositions. The evolution of PCVC is a microcosm of the Central Andean arc in this region where, from 10 to 1 Ma, upper crustal MASH processes resulted in the production and eruption of large volumes of homogeneous crystal-rich dacite during a regional ignimbrite flare-up. Since ∼1 Ma,

* Corresponding author. Tel.: +1 319 335 1828; fax: +1 319 335 1821.
E-mail address: dale-burns@uiowa.edu (D.H. Burns).
[1] Present address: Department of Earth and Environmental Sciences, 115 Trowbridge Hall, University of Iowa, Iowa City, IA 52242, USA.

http://dx.doi.org/10.1016/j.epsl.2015.04.002

decreasing explosivity, smaller eruptive volumes, increasing heterogeneity, and the emergence of less isotopically enriched basaltic-andesite to dacite composite volcanoes signal a return to steady-state arc volcanism.

We posit that the transition from flare-up to steady state captured at the PCVC tracks the waning of the arc scale "thermal engine". High magmatic fluxes during the flare-up would lead to elevated geothermal gradients and efficient crustal processing leading to a dominantly "crustal" magmatism feeding the large volume Purico ignimbrite. This upper crustal MASH zone would act as an efficient filter to any parental compositions precluding them from the eruption record. As magmatic flux and thermal energy wanes, crustal isotherms would relax leading to greater thermal contrast between parental magmas, upper crust, and remnant felsic magmas stored in the upper crust. These changes are manifested in the preservation of textural and compositional heterogeneity and the survival of less isotopically enriched magmas in the upper crust. The chemical imprint of these arc-scale changes in magma dynamics is recorded at all scales from bulk rock to intra-crystalline. The distinct magma dynamics and chemical signatures of the two modes of arc magmatism detailed here should provide a model for investigations of mature continental arc evolution through time and space.

1. Introduction

Continental magmatic arcs exhibit cyclic, episodic behavior (Ducea, 2001; DeCelles et al., 2009). Much of the lifetime of an arc is characterized by steady low-volume magmatism producing composite volcanoes and minor centers and their tonalitic and dioritic plutonic equivalents. This steady state is periodically punctuated by short-lived (∼10–20 Ma) high intensity flare-ups, or high-flux events, during which magma production rates are 3–4 times greater than during the steady state, and cordilleran batholiths and their volcanic equivalents, caldera fields and ignimbrite plateaux form (Lipman et al., 1972; DeCelles et al., 2009; Best et al., 2013). These transient excursions of elevated mantle-to-crust flux are thought to be triggered by major changes in subducting slab–mantle wedge–upper plate architecture (e.g., delamination, slab-rupture, slab steepening) setting up a series of feedbacks that lead to elevated geotherms and prodigious "upper plate" or "crustal" magmatism (de Silva and Gregg, 2014). The space–time–volume character of flare-up episodes defines a broad pulse-like pattern that reflects the topology of the mantle flux and its modulation by the crustal column. A waxing, catastrophic, and waning pattern of volcanism is produced and is thought to reflect the evolving thermal state of the upper crust (de Silva and Gregg, 2014); a model that has been a foundation of our understanding of large silicic magmatic systems for decades.

Volcanic activity during flare-up events is dominated by the eruption of tens-of-thousands of cubic kilometers of ignimbrites and the formation of multiple spatially and temporally related caldera complexes (de Silva et al., 2006; Lipman, 2007; Best et al., 2013). The plutonic systems associated with flare-up magmatism are batholith-scale magma bodies (Lipman et al., 1972; Ducea, 2001), which are essential in the formation of new continental crust (e.g. Johnson, 1991; Ducea, 2001).

Conversely, steady-state magmatism constructs arc composite volcanoes and is characterized by low mantle power input, low magmatic fluxes, and normal geothermal gradients. This manifests as small volume largely effusive eruptions with only occasional explosive caldera forming events (e.g., de Silva, 2008). Eruption volumes and eruptive and magmatic fluxes are typically orders of magnitude lower than during flare-ups (de Silva and Gosnold, 2007) and the chemical character of the eruptive products is typically less evolved and less enriched in crustal components (Ducea and Barton, 2007). Thus, flare-ups are typically distinguishable from steady-state magmatism in both the volcanic and plutonic record by their prodigious volumes, textural and compositional homogeneity, and high crustal affinities (e.g. Lipman et al., 1978; de Silva, 1989; Best et al., 2013). However, while the general characteristics and signatures of flare-up and steady-state magmatism are well characterized and understood independently, there are few studies that address the transition from flare-up to steady-state magmatism as a stage in arc evolution.

Capturing this transition is challenging and has typically been addressed at the regional scale. In an early petrologic investigation of the Southern Rocky Mountain Volcanic Field, Lipman et al. (1978) contrast Oligocene intermediate "flare-up" magmas with distinct upper crustal affinities with later Miocene–Pliocene bimodal volcanism of more mantle affinity, and determined that the switch from flare-up to steady-state magmatism occurred ∼25 Ma and reflects "*a waning thermal environment where crustal geothermal gradients returned to normal steady state*". Johnson (1991) suggested that the transition reflected "basaltification" of the lower crust, but implicit in his models are the change in high to low flux and attendant changes in the geotherm. Ducea and Barton (2007) demonstrate that episodes of high-flux magmatism coincide with negative ε_{Nd} excursions while "normal" arc flux correlates with the opposite characteristics.

Resolution of this transition at a finer scale and placing temporal constraints has been challenging, but we describe here the volcanic and magmatic record of the ∼1 to 0.2 Ma Purico–Chascon Volcanic Complex (PCVC) of the Central Andes. In the subduction-related Central Andes, the transition from steady state to flare-up back to steady state conditions in the Neogene is recorded physically and chemically in the materials produced and erupted during the evolution of the arc. Steady-state magmatism is characterized by predominantly mafic to andesitic volcanism that has less radiogenic $^{87}Sr/^{86}Sr$ ratios <0.708, while the flare-up is dominantly dacitic in composition with more radiogenic "crustal" $^{87}Sr/^{86}Sr$ ratios >0.708. These differences are thought to reflect variable degrees of crustal assimilation in response to changing thermal fluxes (de Silva et al., 2006). We find that the transition from flare-up to steady state happens after 1 Ma and is recorded in whole rock chemical characteristics, mineral phase equilibria, and *in situ* mineral compositional and isotopic data. These datasets provide a time-transgressive view of the upper crustal magma dynamics beneath PCVC that mimics those at the arc scale during the transition.

2. Geologic background

Arc magmatism has occurred continuously in the Central Volcanic Zone (CVZ) of the Andes since ∼200 Ma (e.g., Coira et al., 1982; Rogers and Hawkesworth, 1989) with magmatism migrating eastwards and then back westwards to its current position in response to changes in the dip of the subducting slab (Allmendinger et al., 1997). The westward migration started ∼25 Ma coincident with crustal shortening that continued until at least 10 Ma, re-

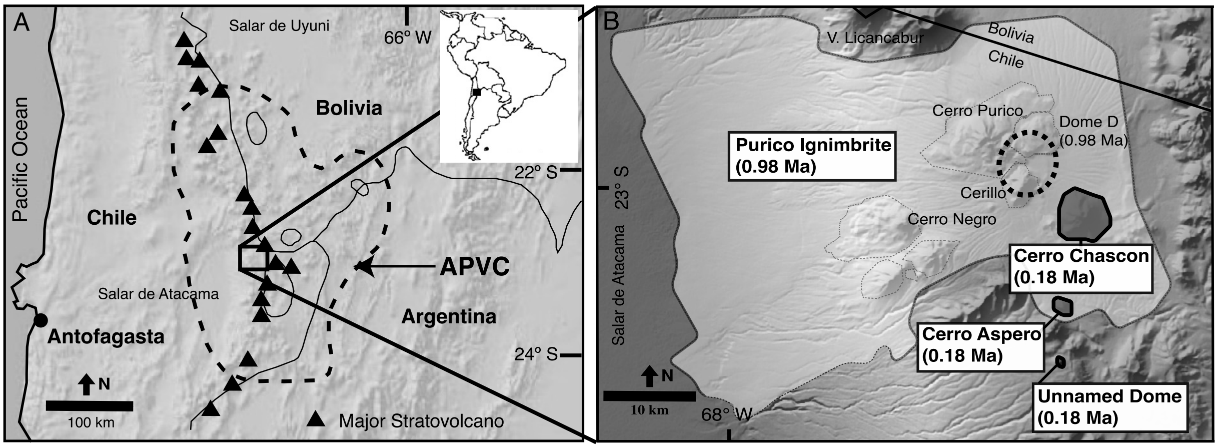

Unnamed d

Fig. 1. Location and context of the Purico–Chascon Volcanic Complex (PCVC) and its components. (A) Map shows the location of the PCVC in northern Chile. The dashed line field shows the extent of the Altiplano–Puna Volcanic Complex (APVC; de Silva, 1989). The irregular ellipses represent the locations of 10–1 Ma APVC caldera complexes (Salisbury et al., 2011), and the black triangles show the location of composite cones that define the modern Central Volcanic Zone (CVZ) arc (from de Silva and Francis, 1991). (B) Detailed map of the Purico–Chascon volcanic complex. The pale field represents the 0.98 Ma Purico ignimbrite (dashed ellipse shows ignimbrite vent), and the dark grey fields show the 0.18 Ma Cerro Aspero and Cerro Chascon lava domes. A small, unnamed third dome in the group is also shown to the south of Aspero.

sulting in crustal thicknesses >70 km beneath the PCVC. The later history of shortening was broadly synchronous with an arc-wide magmatic flare-up that generated significant volumes of "crustal" silicic magma. The most intense surface expression of this is the Altiplano–Puna Volcanic Complex (APVC) between 21° and 24°S (Fig. 1A; de Silva, 1989). Here, from 10 to 1 Ma, inferred magmatic fluxes increased by over an order-of-magnitude relative to steady state CVZ volcanism (de Silva and Gosnold, 2007) resulting in the eruption of >15,000 km^3 of mainly crystal-rich dacitic magma. Activity has waned since 4 Ma and the last major ignimbrite eruption occurred ∼0.7 Ma. A return to steady state conditions is signaled by composite volcanoes, small-volume lava domes, and the appearance of volumetrically dominant andesite (Hawkesworth et al., 1982; de Silva et al., 1994; Watts et al., 1999; Grunder et al., 2008).

The most complete record of this transition is the Purico–Chascon Volcanic Complex (PCVC), the youngest major volcanic center associated with the APVC (Fig. 1). The complex consists of the ∼1 Ma Purico ignimbrite shield (0.98 ± 0.03 Ma; Salisbury et al., 2011), the result of the eruption of ∼80–100 km^3 of crystal-rich, predominantly high-K dacite (rare andesite and rhyolite pumice are limited to one stratigraphic unit). The Purico ignimbrite is physically, texturally, compositionally, and isotopically similar to other large ignimbrites associated with the APVC (Figs. 2–4). The ignimbrite is capped by a summit complex of younger dacite lava domes (<6 km^3), the youngest being the ∼0.18 ± 0.02 Ma Cerro Chascon and Cerro Aspero domes, and a third unnamed dome to the south (Fig. 1B; Hawkesworth et al., 1982; Francis et al., 1984; Davidson et al., 1990; Schmitt et al., 2001; Burns, 2014).

In contrast to the Purico ignimbrite, these younger lava bodies are significantly less voluminous (<6 km^3 in total) and are texturally, compositionally, and isotopically heterogeneous (Figs. 2–4). The domes consist of crystal-rich, high-K dacite lava (Fig. 3) with abundant (up to 20 vol.%) under-cooled basaltic-andesite inclusions (Hawkesworth et al., 1982; Francis et al., 1984; Davidson et al., 1990). The inclusions have the least radiogenic bulk $^{87}Sr/^{86}Sr$ isotopic ratios found in the APVC and are indistinguishable from nearby steady-state arc volcanoes and minor mafic centers of the modern arc (Fig. 4; Feeley and Davidson, 1994; Davidson and de Silva, 1992). The whole rock isotopic composition of the crystal-rich dacite of the Cerro Chascon dome falls on a mixing line between the Purico ignimbrite and basaltic-andesite inclusions (Schmitt et al., 2001; Fig. 4).

3. Petrography

Dacite pumice from the Purico ignimbrite (Fig. 2A, D) is coarse-grained and crystal rich (∼48–59% crystals) consisting of plagioclase (∼35%), amphibole (∼8%), quartz (∼6%), biotite (∼3%), and rare orthopyroxene (<1%), oxides (<1%), and accessory zircon, apatite, and sphene in a groundmass (GM) of fresh, moderately vesicular rhyolite glass (74 wt.% SiO_2). Phenocrysts are generally large (>1 mm), ranging from euhedral to subhedral, and are highly fractured. Disequilibrium textures are restricted to resorbed zones in the interior of plagioclase crystals (<5% of plagioclase crystals).

Dacite lavas from Cerro Chascon (Fig. 2B, E) are also coarse-grained and crystal-rich (∼65% crystals; ∼40% phenocrysts, 15% microphenocrysts), and contain plagioclase (∼20%), quartz (∼6%), amphibole (∼5%), clinopyroxene (∼3%), biotite (∼3%), oxides (∼2%), K-feldspar (<1%), olivine (<0.5%), orthopyroxene (<0.1%), and accessory zircon, apatite, and sphene in a finely crystalline, moderately vesicular groundmass consisting of plagioclase (∼26% of GM) and amphibole (∼24% of GM) microphenocrysts in high-silica rhyolite glass (76 wt.% SiO_2). Phenocrysts are typically large (>1 mm) and range from euhedral to anhedral but are rarely fractured. K-feldspar oikocrysts are up to 5 cm and contain plagioclase, amphibole, biotite, and quartz chadacrysts. Disequilibrium textures are common in the dacite lava and include resorbed quartz with clinopyroxene mantles, dusty sieved plagioclase, and olivine with amphibole rims.

Basaltic-andesite inclusions from Cerro Chascon (Fig. 2C, F) are fine-grained and porphyritic (60–66% crystals; ∼15% phenocrysts, 50–53% microphenocryst) consisting of clinopyroxene (∼5%), amphibole (∼4%), olivine (∼3%), oxides (∼2%), plagioclase (∼1%), and rare quartz (<0.5%) and biotite (<0.1%) in a finely crystalline, moderately vesicular groundmass (27 vol.%) consisting of plagioclase (43–44% of GM) and amphibole (32–33% of GM) microphenocrysts in rhyolite glass (75 wt.% SiO_2). Phenocrysts are typically large (>1 mm) subhedral to anhedral, and out of equilibrium with the groundmass glass. Disequilibrium textures are prevalent and are similar to textures in the Cerro Chascon dacite including resorbed quartz with clinopyroxene mantles, dusty sieved plagioclase, and olivine with amphibole rims. Importantly, all of the phenocrysts

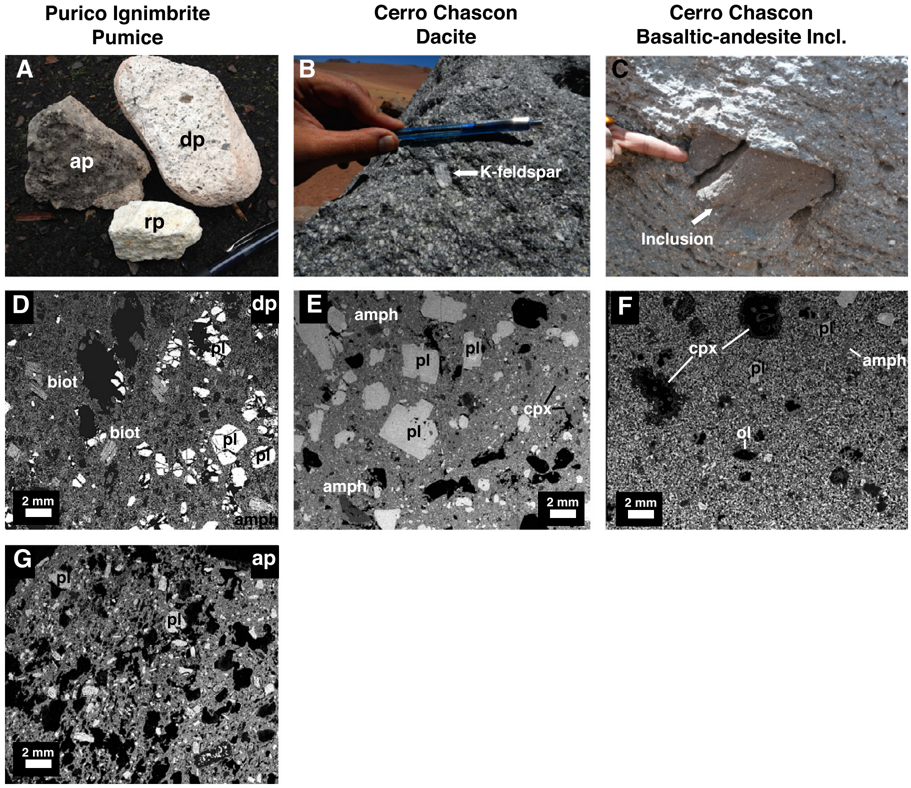

Fig. 2. Field and microscopic textural features of the main lithologies of the Purico–Chascon Volcanic Complex (PCVC). (A–C) Field photographs and (D–G) Al X-ray maps of pumice from the Purico ignimbrites (rp: rhyolite pumice; dp: dacite pumice; ap: andesite pumice), and the host dacite lava and basaltic-andesite inclusions from Cerro Chascon. Note the increasing textural maturity between the Purico ignimbrite dacite pumice and the Cerro Chascon dacite lava and the large K-feldspar oikocryst in the latter. Select crystalline phases (plagioclase-plag; amphibole-amph; biotite-biot, clinopyroxene-cpx; olivine-ol) are labeled to show how their textures change throughout the units. CPX, highlighted in the basaltic-andesite inclusion (F), forms reaction rims on remnant quartz xenocrysts.

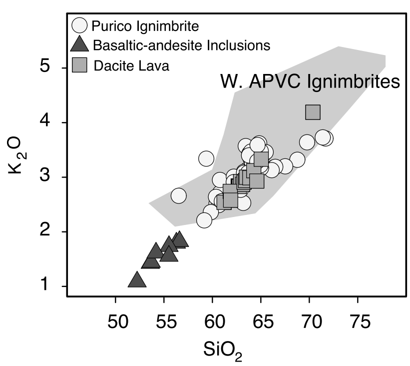

Fig. 3. SiO_2 vs. K_2O comparing crystal-rich host and mafic inclusions from Cerro Chascon with pumice from the Purico and western APVC ($n = 73$) ignimbrites. The composition of the crystal-rich host is dacite, whereas, the mafic inclusions are basaltic-andesite. Note the large compositional gap between the inclusions and host from Cerro Chascon. Data sources: Hawkesworth et al. (1982), de Silva (1991), Schmitt et al. (2001), Lindsay et al. (2001), de Silva and Gosnold (2007), Kay et al. (2010).

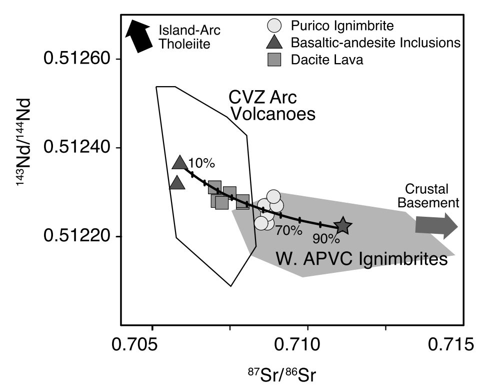

Fig. 4. Isotopic characteristics of the Purico–Chascon Volcanic Complex (PCVC). Bulk rock $^{87}Sr/^{86}Sr$ vs. $^{143}Nd/^{144}Nd$ from the Purico ignimbrite and Cerro Chascon lavas with 1 Ma to recent (steady-state) lavas and tuffs from the CVZ (white field; $n = 306$) and ignimbrites of the western APVC (grey field; $n = 28$) for reference. Black curve shows modeled isotope mixing hyperbola for the PCVC. Tick marks are at 10% intervals with the star representing the crustal end-member (Schmitt et al., 2001), and the basaltic-andesite inclusions as the parent. The end-member(s) details are presented along with the mixing solutions in the supplementary data tables. Data sources: Hawkesworth et al. (1982), de Silva (1991), Schmitt et al. (2001), Lindsay et al. (2001), Kay et al. (2010). See supplementary materials for isotope data tables.

observed in the mafic inclusions show signs of disequilibrium. Microphenocrysts in the inclusions are typically small (<0.5 mm) and appear to be in equilibrium with the groundmass glass.

Two striking petrographic features of rocks from the PCVC are the physical and textural similarity between individual phenocrysts from all three units and the general trend of increasing in textural maturity (coarseness) between the Purico ignimbrite and Cerro Chascon dacite (Fig. 2). Phenocrysts from the Cerro Chascon dacite have similar textures and sizes as crystals from the Purico ignimbrite. However, plagioclase crystals in the Purico ignimbrite occur exclusively as individual crystals sitting in groundmass glass, whereas, plagioclase in the Cerro Chascon dacite often occur in clumps of two or more crystals annealed to one another.

The Cerro Chascon dacite also contains K-feldspar oikocrysts. The oikocrysts are large (up to 5 cm) and include the same phenocrysts as the dacite lava groundmass and the Purico ignimbrite pumice. The oikocrysts display rapakivi texture (plagioclase rims) and the interiors are homogeneous K-feldspar and lack perthitic textures indicating that the magma in which they were hosted

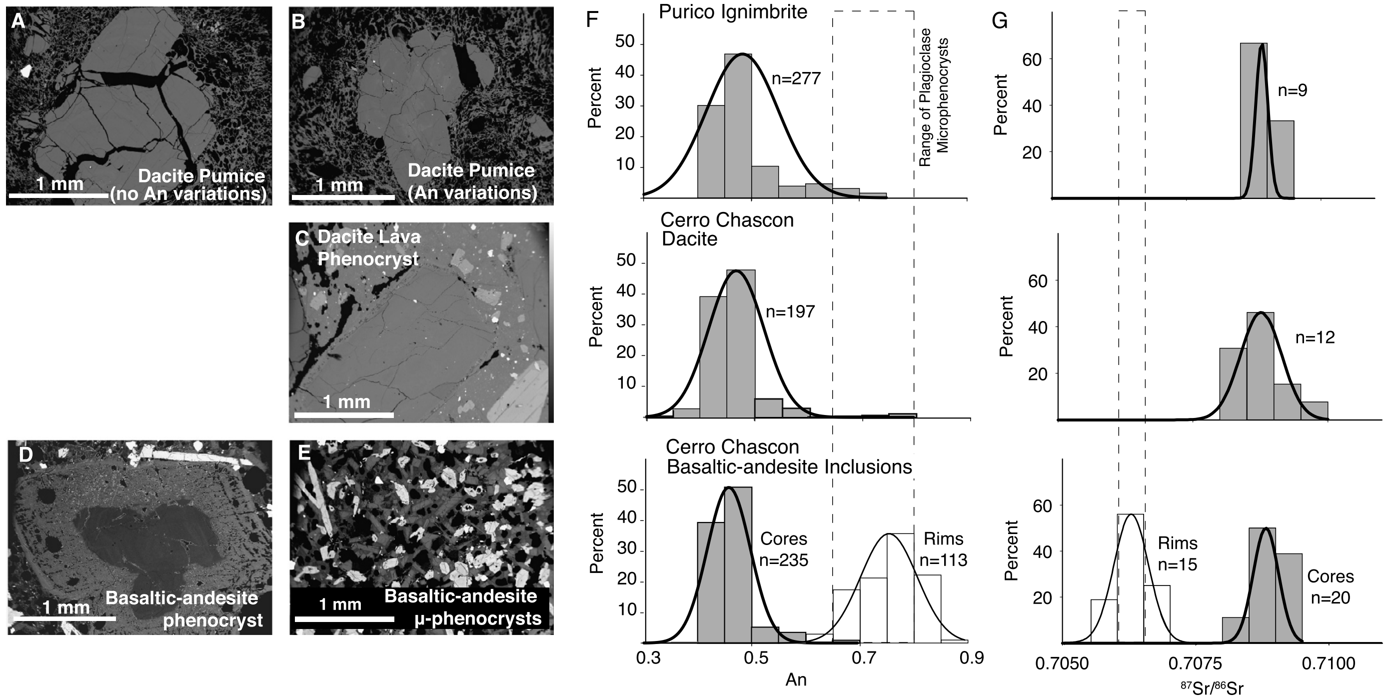

Fig. 5. Petrographic features and *in situ* chemistry of plagioclase from the Purico–Chascon Volcanic Complex (PCVC). (A–E) Back-scattered electron images show the characteristic plagioclase populations from the Purico ignimbrite dacite pumice (A, B) and Cerro Chascon dacite (C) and basaltic-andesite inclusions (D, E). Note the similarity in plagioclase phenocryst sizes in all three eruptive units. Also note the clear disequilibrium textures in phenocrysts from the basaltic-andesite inclusion (D). (F) Histograms show anorthite contents of plagioclase crystals from the units discussed above. Plagioclase cores and rims from phenocrysts within the basaltic-andesite inclusions are plotted separately. The dashed box shows the composition(s) of plagioclase microphenocrysts in the Cerro Chascon basaltic-andesite inclusions. (G) Histograms of $^{87}Sr/^{86}Sr$ isotope ratios for the units described above. Plagioclase phenocryst cores and rims from Cerro Chascon basaltic-andesite inclusions are plotted separately. Symbols, fields, and Gaussian curves are the same as in (F). The scale for all histograms and Gaussian distribution curves is relative probability. Complete major element and isotopic datasets are available in the supplementary materials.

never cooled below ∼600 °C (Bowen and Tuttle, 1950). Similar K-feldspar oikocrysts have been found in other lava domes in the APVC and have been interpreted as late-stage crystallization during the early stages of pluton formation (Watts et al., 1999). The rapakivi textures are commonly ascribed to dissolution and sanidine–melt interactions during mafic recharge (Vernon, 1986).

Disequilibrium textures in the Cerro Chascon lavas clearly record evidence of mafic recharge (see Davidson et al., 1990). The similarity between crystals in the Purico ignimbrite and Cerro Chascon lavas and the lack of perthitic textures in K-feldspar oikocrysts, and their rapakivi texture are consistent with the remobilization of remnant, near-solidus (>600 °C) Purico ignimbrite crystal mush during the intrusion of the basaltic-andesite magma. In order to understand the textural–compositional–isotopic relationships between the crystalline phases in the PCVC and how they relate to the long-term evolution of the PCVC, and the CVZ as a whole, we measured *in situ* major element abundance and isotope ratios of plagioclase.

4. Analytical methods

In situ major and trace element abundances were measured via electron microprobe (EMP) using a Cameca SX100 electron microprobe at Oregon State University (OSU). Detailed run conditions, calibration procedures, and analytical errors are presented in the supplementary materials. *In situ* isotopic analyses where conducted using two methods. Selected crystals were sampled using a NuWave computer-automated micro-drill at OSU and sampled aliquots were sent to New Mexico State University (NMSU) where elemental Sr was separated using cation-exchange chromatography. $^{87}Sr/^{86}Sr$ was then measured using thermal ionization mass spectrometry (TIMS) at NMSU. *In situ* isotopic analyses were also measured using a NuPlasma multi-collector inductively coupled plasma mass spectrometer MC-ICP-MS and Photon Machines G2 Excimer laser system in the W.M. Keck Collaboratory for Mass Spectrometry at OSU. Detailed comparison of the two methods along with analytical methods for LA-ICP-MS analyses are discussed in the supplementary materials.

5. Crystal chemistry

5.1. Plagioclase

Plagioclase crystals from the Purico ignimbrite typically have relatively low anorthite ($An_{40–55}$) and MgO contents (<200 ppm; Fig. 5A, F; Table 1) and high, restricted $^{87}Sr/^{86}Sr$ isotope ratios (0.7087–0.7090; Fig. 5G). The rare crystals with resorbed surfaces have cores that define a much broader range in An ($An_{39–85}$; Fig. 5B, F). However, these crystals show no significant core to rim differences in MgO content or $^{87}Sr/^{86}Sr$ isotope ratios (Fig. 5F).

Plagioclase phenocrysts from the Chascon dacite (Fig. 5C) have low anorthite (∼80% of analyses between $An_{40–55}$; Fig. 5F) and MgO contents (<200 ppm) similar to the Purico ignimbrite. Isotopically, phenocryst interiors have slightly more variable $^{87}Sr/^{86}Sr$ ratios, but they overlap with the Purico ignimbrite (0.7083–0.7095; Fig. 5G). In contrast to the plagioclase in the ignimbrite, these crystals show significant rim-ward increases in An and MgO ($An_{65–80}$ and 500–800 ppm MgO, respectively) and decreases in $^{87}Sr/^{86}Sr$ (0.7065–0.7072; Fig. 5F, G; Table 1).

Basaltic-andesite inclusions from Cerro Chascon contain two distinct types of plagioclase (Fig. 5D, E). Phenocrysts with dusty sieved textures have clear cores with low An and MgO contents ($An_{39–55}$ and <200 ppm, respectively) and high $^{87}Sr/^{86}Sr$ ratios (0.7085–0.7091; Fig. 5D, F, G; Table 1). Dusty sieved zones and clear growth rims surrounding the sieved zone have significantly higher An and MgO contents ($An_{65–85}$ and 400–800 ppm MgO)

Table 1
Summary of plagioclase and amphibole textures and compositions.

Plagioclase						
Unit	Purico ignimbrite	Cerro Chascon				
Rock type	Dacite pumice	Dacite lava		Basaltic-andesite inclusions		
	Plag. phenocrysts	Plag. phenocrysts		Plag. phenocrysts		Plag. µphenocrysts
Size (µm)	500–1500	500–1500		500–1500		< 500
Shape	subhedral	euhedral/subhedral		subhedral/anhedral		subhedral
	Cores & rims	Cores	Rims	Cores	Rims	Cores & rims
Texture	clear	clear	clear/sieved	clear	sieved	clear
An	40–55	40–55	65–80	39–55	65–85	64–84
MgO (ppm)	<200	<200	500–800	<200	400–800	500–800
$^{87}Sr/^{86}Sr$	0.7087–0.7090	0.7083–0.7095	0.7065–0.7072	0.7085–0.7091	0.7057–0.7065	0.7062–0.7064

Amphibole					
Unit	Purico ignimbrite	Cerro Chascon			
Rock type	Dacite pumice	Dacite lava		Basaltic-andesite inclusions	
Classification[a]	Mg-hornblende	Mg-hornblende	Tschermakite	Mg-hornblende	Tschermakite
Size	>1 mm	>1 mm	<0.5 mm	>1 mm	<0.5 mm
Texture	clear	clear	clear	clear	clear
SiO_2	45.20–49.62	46.02–49.41	45.22–49.62	45.20–48.31	45.22–49.62
Al_2O_3	6.24–9.90	6.57–8.49	11.25–14.28	8.18–8.15	12.08–13.97
^{IV}Al	1.03–1.49	1.11–1.38	1.29–2.15	1.26–1.29	1.84–2.03
Ti^C	0.11–0.25	0.08–0.14	0.11–0.32	0.09–0.13	0.17–0.22
Mg#	0.59–0.69	0.58–0.63	0.60–0.71	0.60–0.69	0.67–0.72
^TSi	6.51–6.97	6.62–6.89	5.85–6.71	6.71–6.74	5.97–6.16
T (°C)[b]	788–874	796–841	928–1001	827–891	943–985
P (MPa)[c]	85–205	94–153	319–580	141–185	346–550
Depth (km)[d]	4–8	4–6	12–22	5–7	13–21

[a] Leake et al. (1997).
[b] Ridolfi et al. (2010), Holland and Blundy (1994).
[c] Ridolfi et al. (2010), Anderson and Smith (1995).
[d] Ridolfi et al. (2010).

with lower $^{87}Sr/^{86}Sr$ ratios (0.7057–0.7065). Plagioclase microphenocrysts (Fig. 5E) in the inclusions have high An and MgO contents ($An_{64–84}$ and 500–800 ppm MgO; Fig. 5F) and low, restricted $^{87}Sr/^{86}Sr$ ratios (0.7062–0.7064; Fig. 5G) similar to the outermost rims of the larger crystals.

5.2. Amphibole

Amphibole crystals in the PCVC can be divided into two distinct groups based on their size and major element compositions (Fig. 6A, B, C; Table 1). Large (typically >1 mm) low-Al amphiboles found in the Purico ignimbrite and lavas (dacite and basaltic-andesite inclusions) from Cerro Chascon (Fig. 6A, C) have relatively low Al_2O_3 (6.24–9.90 wt.%) with high SiO_2 (45.20–49.62 wt.%). Site-specific cation abundances calculated using the methods outlined by Leake et al. (1997) are presented in Fig. 6D–F and show that low-Al amphiboles have relatively low ^{IV}Al, ^{C}Ti, Mg# [Mg/(Mg + Fe^{2+})] and high ^{T}Si (Table 1). Following the classification scheme of Leake et al. (1997) the amphiboles are magnesiohornblendes (Fig. 6D). There are no systematic compositional differences between cores and rims in these crystals. Rims differ by $\sim\pm1$ wt.% Al_2O_3 compared with crystal cores and many amphiboles have cores and rims that are indistinguishable. Similarly, SiO_2, ^{IV}Al, ^{C}Ti, and Mg# do not vary systematically between cores and rims.

Cerro Chascon lavas (dacite and basaltic-andesite inclusions) contain a second population of high-Al amphibole (Fig. 6B, C) not found in the Purico ignimbrite. These crystals are significantly smaller (<0.5 mm) with higher Al_2O_3 (11.25–14.28 wt.%) and lower SiO_2 (45.20–49.62 wt.%) than the low-Al magnesiohornblendes. These high-Al amphiboles also have significantly higher ^{IV}Al, ^{C}Ti, and Mg#, and lower ^{T}Si (Fig. 6D–F; Table 1) and are classified as tschermakites (Leake et al., 1997; Fig. 6D–F). Similar to the magnesiohornblendes, these crystals show no systematic core to rim variations in major elements or cation abundances.

An important observation is that the two amphibole populations form distinct groups in major element space separated by $\sim$3 wt.% Al_2O_3 (Fig. 6C). In addition, significant differences in site-specific cation abundances are consistent with amphibole populations that grew at distinct pressures and temperatures (e.g., Holland and Blundy, 1994; Anderson and Smith, 1995; Ridolfi et al., 2010). In the following section, we investigate the relationships between amphibole compositions and crystallization pressures and temperatures for the Purico ignimbrite and Cerro Chascon lavas and show how the crystallization conditions change over the history of the PCVC.

6. *P*–*T* conditions

6.1. Magmatic temperatures

Magmatic temperatures were estimated using the amphibole thermobarometer of Ridolfi et al. (2010) and the plagioclase–amphibole thermometer of Holland and Blundy (1994) (Fig. 7). Low-Al magnesiohornblendes from the Purico ignimbrite and Cerro Chascon lavas yield temperatures between 788 and 874 ± 25 °C (Ridolfi et al., 2010), similar to temperatures of 795 to 830 °C obtained from Fe–Ti oxide equilibria for the Purico ignimbrite and Chascon dacite (de Silva, 1991; Schmitt et al., 2001; Abot, 2009). In contrast, high-Al tschermakites from Cerro Chascon modeled using the amphibole thermobarometer of Ridolfi et al. (2010) yield significantly higher temperatures (928–1001 ± 25 °C). To verify the

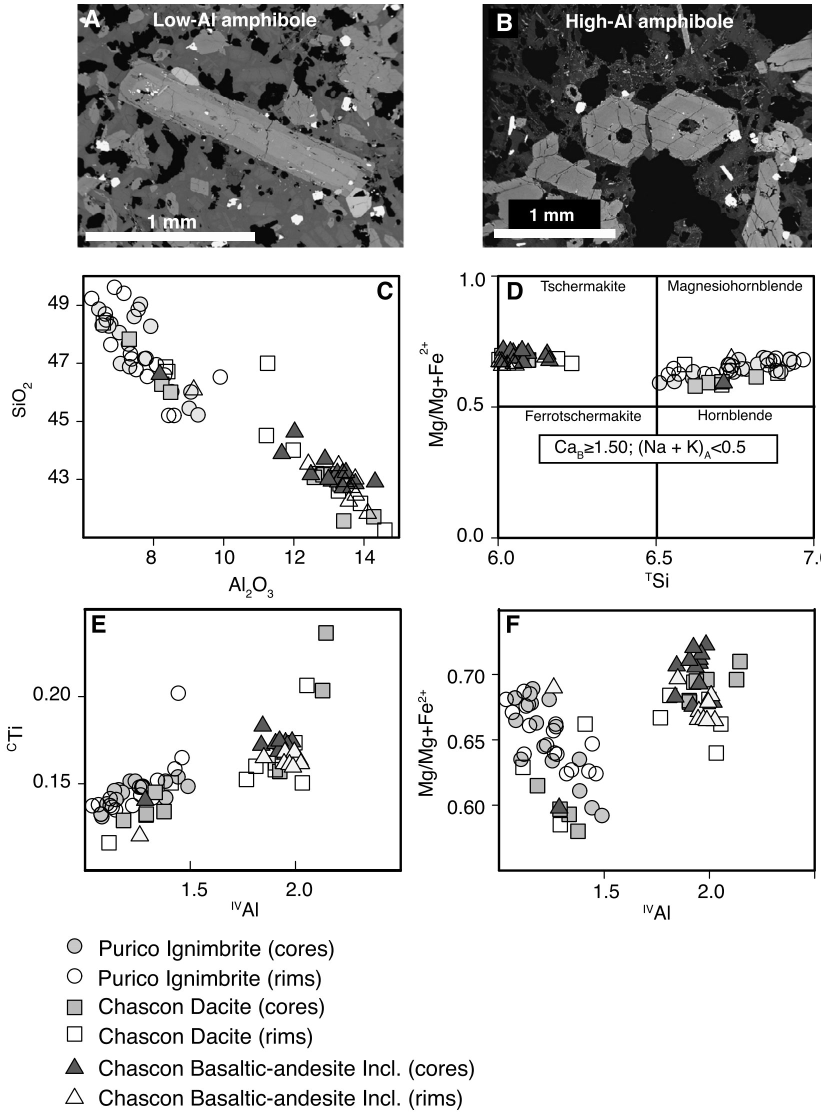

Fig. 6. Petrographic characteristics and compositional data from amphibole from the Purico–Chascon Volcanic Complex (PCVC). (A) Back-scattered electron images of low-Al. (B) Back-scattered electron images of high-Al amphibole crystals. (C) Al_2O_3 vs. SiO_2 diagram comparing high and low-Al amphiboles from the Purico ignimbrite and Cerro Chascon lavas. Note the similarity between low-Al amphibole in the Purico ignimbrite pumice and Cerro Chascon lavas and the compositional gap between high- and low-Al amphiboles (∼9–12 wt.% Al_2O_3). (D) Amphibole classification diagram following Leake et al. (1997) shows Si per formula unit vs. Mg# [Mg/(Mg + Fe^{2+})]. (E, F) Diagrams show tetrahedral coordinated Al vs Mg# and Ti in the c-lattice site. Note the large compositional gaps between the two groups indicating the two amphibole types grew in distinct pressure–temperature environments. Complete dataset presented in the supplementary materials.

temperatures calculated using the model of Ridolfi et al. (2010) magmatic temperatures were also calculated using the edenite–richterite exchange thermometer of Holland and Blundy (1994) for touching plagioclase–amphibole microphenocryst pairs (Fig. 7). Temperatures calculated using this method (925–973 ± 40 °C) are indistinguishable (within uncertainty limits) from temperature estimates calculated using the Ridolfi et al. (2010) model.

6.2. Magmatic pressures

To determine magmatic pressures from the PCVC, we utilize the thermobarometer of Ridolfi et al. (2010). Recently, amphibole crystallization pressures determined using the amphibole thermobarometer of Ridolfi et al. (2010) and Ridolfi and Renzulli (2012) have been under scrutiny. We address these potential issues and justify our use of the Ridolfi et al. (2010) barometer in Supplementary Appendix B. To validate the pressures calculated for the PCVC using Ridolfi et al. (2010), we compare them with pressures modeled using the Al-in-amphibole barometer of Anderson and Smith (1995) and pressure estimates made by Schmitt et al. (2001) using melt inclusion volatile barometry. When multiple barometers are not available we integrate petrographic observations and crystal chemistry with data from pressure-controlled crystallization experiments (Blatter et al., 2013).

Low-Al magnesiohornblendes from the Purico ignimbrite and Cerro Chascon crystallized between 85 and 205 ± 15 MPa (Ridolfi et al., 2010). These pressures are similar to pressures reported by Abot (2009) and Schmitt et al. (2001) for the Purico ignimbrite using the Al-in-amphibole barometer of Anderson and Smith (1995; 70–200 MPa and 150–160 MPa, respectively). These pressures are also similar to pressures reported from other large ignimbrites in the Central Andes (∼100–200 MPa; Folkes et al., 2011).

In contrast, high-Al tschermakites from the Cerro Chascon lavas yield significantly higher pressures (396–580 MPa), with 80% of crystals between 396 and 550 MPa. Al-in-amphibole pressures were not calculated for the high-Al tschermakites as their crystallization temperatures far exceeded the temperatures at which the Anderson and Smith (1995) barometer is calibrated. However, petrographic and compositional data from the Cerro Chas-

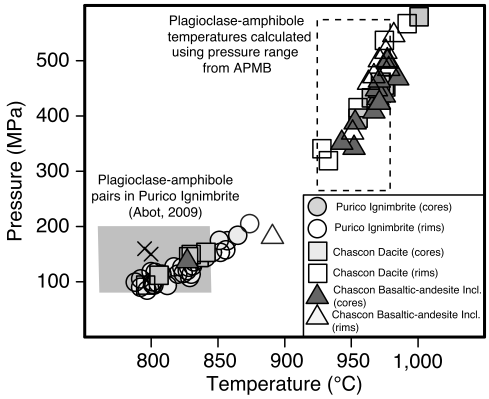

Fig. 7. Magmatic temperatures and pressures calculated for the Purico ignimbrite and Cerro Chascon lavas using a variety of geothermobarometers. Individual points represent estimates based on averages of multiple analyses within the core or rim region of individual crystals (see supplementary data) using the geothermobarometer of Ridolfi et al. (2010). The grey field represents plagioclase–amphibole temperatures and Al-in-amphibole pressures modeled for the Purico ignimbrite dacite pumice by Abot (2009) using the formulations of Holland and Blundy (1994) and Anderson and Smith (1995), respectively. The dashed field represents plagioclase–amphibole temperatures (Holland and Blundy, 1994) estimated over a range of pressures consistent with the APMB (Ward et al., 2014). The X symbols represent magmatic temperatures and pressures for the Purico dacite pumice estimated by Schmitt et al. (2001). Data sources: Ward et al. (2014), Schmitt et al. (2001), Abot (2009).

con basaltic-andesite support these pressures. Petrographically, the olivine–clinopyroxene–plagioclase–amphibole crystallization sequence (Burns, 2014) recorded in the basaltic-andesite inclusions is consistent with 400 MPa hydrated arc basalt crystallization experiments conducted by Blatter et al. (2013). In addition, Blatter et al. (2013) observes that at 400 MPa, ∼45% crystallization of plagioclase (An_{72}) results in a systematic increase in melt H_2O content and the appearance of high-Al (14.7 wt.% Al_2O_3) amphibole on liquidus at ∼1000 °C. The compositional range of high-An plagioclase ($An_{72–84}$) in the Cerro Chascon lavas overlap with the experimental compositions. High-Al amphiboles from Cerro Chascon have slightly lower Al contents than the experimental amphiboles (11.25–14.28 vs. 14.7 wt.% Al_2O_3), which we interpret as slightly lower crystallization temperatures (∼80 °C lower than the experimental amphibole). Importantly, the 45% plagioclase crystallization reported by Blatter et al. (2013) is nearly identical to the 43–44% plagioclase observed in the groundmass of the Cerro Chascon basaltic-andesite. Thus, in the Purico Complex, the tschermakite amphiboles record a deeper origin than the magnesiohornblendes.

7. The story in the crystals: magma dynamics at the Purico–Chascon volcanic complex

Low-Al magnesiohornblendes in the ∼1 Ma Purico ignimbrite record crystallization in a cool (∼790–870 °C) upper crustal (4–8 km depth) magma. Plagioclase crystals from the Purico ignimbrite have high, relatively restricted $^{87}Sr/^{86}Sr$ isotope ratios (0.7087–0.7090) indicating that the ∼1 Ma dacite was significantly "crustal". Conversely, crystals from 0.18 Ma Cerro Chascon dome records two distinct magmatic environments. High $^{87}Sr/^{86}Sr$ plagioclase crystals and low-Al amphiboles in both the dacite and basaltic-andesite inclusions are texturally, compositionally, and isotopically identical to crystals from the Purico ignimbrite and are interpreted to have grown in a similar low temperature (∼800–890 °C), upper-crustal (4–8 km depth) dacite reservoir. In contrast, low $^{87}Sr/^{86}Sr$ plagioclase microphenocrysts from the basaltic-andesite inclusions and high-Al tschermakitic amphibole grew from more mafic magmas at greater depths, between 20 and 15 km. These data allow us to construct a time-transgressive cross section of the magma dynamics beneath the PCVC to show how magma generation, accumulation, and storage changed over the ∼800 kyr history of the PCVC (Fig. 9).

The upper crustal character of the Purico ignimbrite coupled with its radiogenic (high) Sr-isotope ratios indicates magma generation in the upper crust. A lack of heavy REE depletion (no garnet signature), and low (<1) Sr bulk distribution coefficients (below plagioclase stability) in the Purico ignimbrite elucidate extensive MASH processes (∼50–70% assimilation; Fig. 4) between ∼30 and 20 km depth (Schmitt et al., 2001). Rare andesite pumice in the Purico ignimbrite, interpreted by Schmitt et al. (2001) to represent a recharge magma, records a higher temperature (965 °C) deeper upper crustal (∼20–17 km depth) magma reservoir (Schmitt et al., 2001) at depths consistent with a regional low gravity anomaly and low-velocity zone thought to represent the Altiplano–Puna Magma Body (APMB; Chmielowski et al., 1999; de Silva et al., 2006; Ward et al., 2014). The radiogenic character of the andesitic pumice ($^{87}Sr/^{86}Sr$; 0.7085 and 0.7090; de Silva, 1991; Schmitt et al., 2001) suggests that ∼1 Ma the isotopic signature of at least some of the APMB was >0.708. Our data indicate that the APMB magmas ascended to, accumulated, and crystallized at between 4 and 8 km prior to eruption.

Approximately 800 kyr later, the 0.18 Ma Cerro Chascon, and the virtually identical Cerro Aspero and another small unnamed lava dome to the south, record a major change in the magma dynamics below the PCVC. Two compositionally and isotopically distinct magma reservoirs were operating in the upper crust (Fig. 9). The shallow reservoir (4–8 km) is mineralogically, compositionally and isotopically indistinguishable from the Purico ignimbrite magma reservoir. The deeper "APMB" at this time is represented by basaltic-andesite inclusions, plagioclase microphenocrysts, high-Al amphiboles, and lower $^{87}Sr/^{86}Sr$ isotope ratios (0.7057–0.7065) that are clearly distinguishable from the relatively enriched ($^{87}Sr/^{86}Sr$; 0.7085–0.7090) isotopic composition of the APMB and upper crustal dacites at ∼1 Ma.

Davidson et al. (1990) proposed that the basaltic-andesite inclusions in Cerro Chascon and Aspero represent a basaltic-andesite magma that melted and mixed with the Purico ignimbrite to produce a hybrid Chascon dacite. Our observations of increased textural coarseness in the Chascon dacite compared to the Purico ignimbrite pumice and the presence K-feldspar oikocrysts within the Chascon dacite suggest that during the time of the recharge event, a near-solidus crystal mush, probably remnant Purico ignimbrite-producing magma, was present in the upper crust. The Chascon dacite (and Aspero) is therefore seen as the "revived" crystal mush motivated by recharge by basaltic-andesite that had crystallized extensively at APMB depths. Crystallization of the basaltic-andesite between ∼17 and 20 km is recorded in petrographic relationships, high-An plagioclase, and high-Al amphibole compositions.

8. The transition from flare-up to steady-state arc magmatism in the Purico–Chascon volcanic complex

Previous work has established that the 10 to 1 Ma APVC ignimbrite flare-up was characterized by dacitic magmas with strong "crustal" affinity (de Silva, 1989; Ort et al., 1996; Lindsay et al., 2001; de Silva et al., 2006; Kay et al., 2010). These have significantly higher $^{87}Sr/^{86}Sr$ isotope ratios than typical steady state CVZ lavas (Fig. 8A; compiled from Mamani et al., 2010). Bulk pumice from the 1 Ma Purico ignimbrite is isotopically indistinguishable from other APVC ignimbrites (Fig. 8A, B; de Silva, 1991; Lindsay et al., 2001; Schmitt et al., 2001; Kay et al., 2010). Here we have shown that individual plagioclase crystals from the Purico ignimbrite are also isotopically identical to bulk rock isotopic measurements from the ignimbrite pumice; the elevated isotopic signal

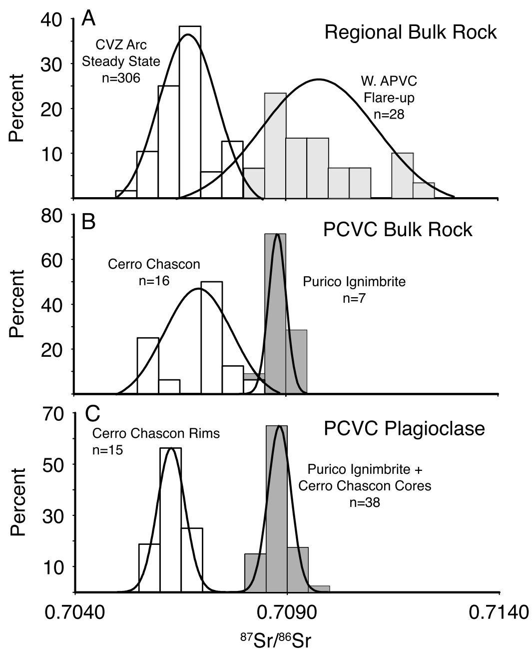

Fig. 8. Comparison of regional (arc-wide) bulk rock isotopic data with bulk rock and *in situ* isotopic data from the Purico–Chascon Volcanic Complex (PCVC). (A) Histogram shows bulk rock $^{87}Sr/^{86}Sr$ isotope ratios of ignimbrites of the W. APVC and lavas and tuffs from the steady state (1 Ma–recent) CVZ arc. Gaussian distribution curves (black curves) in all panels are calculated for the data shown in histograms. (B) Histogram of bulk rock $^{87}Sr/^{86}Sr$ isotope ratios for units of the PCVC. Data from the Cerro Chascon dacite lava and basaltic-andesite inclusions are combined. (C) Histogram of $^{87}Sr/^{86}Sr$ isotope ratios from plagioclase crystals in the PCVC. Plagioclase phenocrysts from the Purico ignimbrite, Cerro Chascon dacite lava, and plagioclase phenocryst cores from Cerro Chascon basaltic-andesite inclusions are combined. The scale for all histograms and Gaussian distribution curves is relative probability. Data sources are presented in Fig. 4.

of the APVC flare-up is thus also recorded at the crystal scale (Fig. 8C).

In addition to the elevated radiogenic isotope ratios, the isotopic homogeneity of the pumice and crystals from the Purico ignimbrite are evidence that these are "flare-up" magmas. During the APVC flare-up, extensive crustal assimilation and fractional crystallization in the upper crust between 35 and 15 km depth (the crust beneath the APVC being 70 to 80 km thick) led to the generation of large amounts of isotopically enriched magma ($^{87}Sr/^{86}Sr$ = 0.7080–0.7132; Schmitt et al., 2001; Fig. 9). During this time, magmas were being supplied to the uppermost crust from the APMB (Chmielowski et al., 1999; de Silva et al., 2006). Data from APMB dacites and andesites from other centers in the APVC are consistent the APMB being largely upper crustal in its isotopic character ($^{87}Sr/^{86}Sr$ >0.708; e.g. de Silva, 1991). More "parental" baseline compositions ($^{87}Sr/^{86}Sr$ ∼0.705 to 0.706) were likely still being supplied from below, but that signal was being filtered out by the vigorous upper crustal system (e.g., Bachmann and Bergantz, 2008). Thus, during the flare-up, the APMB was an intermediate "mothership", a vertically extensive upper crustal MASH zone parental to the shallower, pre-eruptive, dacite magma reservoirs that have erupted within the footprint of the APVC. Once established, the APMB would have buffered the composition(s) of magmas by trapping ascending mafic magmas to offset extensive fractionation and assimilation. Development of the APMB was the primary influence on the thermomechanical evolution of the upper crust during the ignimbrite flare-up essentially conditioning the crust above it for growth of the large pre-eruptive dacitic chambers like that of the Purico ignimbrite (de Silva and Gosnold, 2007; de Silva and Gregg, 2014). Differentiation to more crustal isotopic ratios >0.708 indicate further assimilation at the shallowest levels

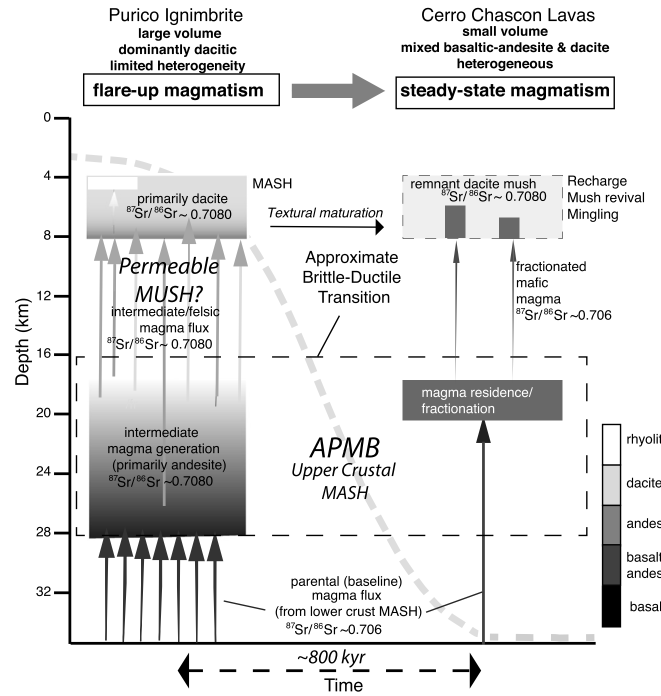

Fig. 9. Schematic time-trangressive cross-section of magma dynamics at the Purico–Chascon Volcanic Complex (PCVC). This depicts in a heuristic and phenomenological way how the generation, transportation, and storage of magmas changed throughout the history of the PCVC, and how those changes reflect changes in the regional geothermal gradient. Vertical arrows in the foreground show the composition (see composition legend in lower right), ascent path, and relative flux of magmas with density of flow paths representing relative flux. Shaded boxes show the locations of magma accumulation and compositions of accumulating magmas with shading representing composition. Horizontal arrows show how processes at a specific level in the crust evolve with time and waning thermal flux represented by the brittle–ductile transition curve (based on de Silva and Gosnold, 2007) throughout the evolution of the PCVC. Note that during the development and eruption of the Purico ignimbrite (∼1.0 Ma), the thermal flux was high and significant upper crustal MASH controlled the composition of magmas erupting on the surface. In contrast, during the ascent of the Cerro Chascon magmas, the thermal flux was low and parental mafic magmas ascended from depth into the upper crust with no significant mid-crustal interactions.

and we envisage that MASH processes were occurring in the shallow pre-eruption chambers albeit at lower intensity than in the APMB (Fig. 9).

The small volume, effusive, bimodal character of Cerro Chascon and Aspero is in marked contrast to the flare-up ignimbrites and signals the return to steady-state arc magmatism. The basaltic-andesite inclusions are similar to mafic inclusions found in other arc settings (e.g. Eichelberger, 1980; Tepley et al., 1999) and are the most mafic and "primitive" compositions recorded in the APVC. They have the lowest $^{87}Sr/^{86}Sr$ isotope ratios in the APVC (Fig. 4, Fig. 8A, B) and are identical to the range of isotope ratios observed in recent CVZ arc lavas (Mamani et al., 2010) and small back-arc centers on the Bolivian Altiplano (Davidson and de Silva, 1992). The basaltic-andesite inclusions attest to a change in the APMB to a zone with more mafic compositions than during the flare-up. Their isotopic character is close to the most non-radiogenic Sr isotopic signatures from the Central Andes (∼0.705–0.706), which was proposed to be the regional isotopic baseline composition by Davidson et al. (1991). These have been attributed to both enriched mantle compositions (e.g. Rogers and Hawkesworth, 1989; Kay et al., 2010) and lower crustal assimilation and MASH (Davidson et al., 1991). We do not try to distinguish between these models, but note that the low $^{87}Sr/^{86}Sr$ ratios of Cerro Chascon basaltic-andesite inclusions attest to significantly less crustal processing relative to the magmas feeding the APVC ignimbrites.

The characteristics of the dacite lava of Cerro Chascon are consistent with it representing a hybrid of remnant Purico ignimbrite mush and more primitive basaltic-andesite from the APMB. In $^{87}Sr/^{86}Sr$ vs. $^{143}Nd/^{144}Nd$ space, the bulk isotopic characteristics clearly define an array between the Purico ignimbrite and the basaltic-andesite (Fig. 4). At the crystal-scale, amphibole and plagioclase phenocrysts record P–T conditions and isotopic compositions of the flare-up (the Purico ignimbrite). On the other hand, amphibole microphenocrysts attest to depths of equilibration in the APMB (Fig. 5G, Fig. 8A, B). Crystal cores record elevated $^{87}Sr/^{86}Sr$ ratios associated with the flare-up, and rims record much lower $^{87}Sr/^{86}Sr$ ratios characteristic of steady-state CVZ arc (Fig. 8A, C). These attest to the Purico mush being invaded by melts of basaltic-andesite resulting in rims on plagioclase of more An-rich and primitive compositions.

The preservation of textural and chemical heterogeneities in the Cerro Chascon system indicates that the magmas did not thoroughly mix prior to eruption, a common feature of arc-related rocks (e.g. Davidson and Tepley, 1997; Tepley et al., 1999). Instead, injection of the mafic magma into the near-solidus remnant Purico magma reservoir likely triggered an eruption interrupting the mixing processes before the magmas could homogenize. The basaltic-andesite inclusions and plagioclase microphenocrysts from Cerro Chascon record very little isotopic modification in the upper crust. We interpret this as signaling that conditions in the crust were not conducive to producing significant "crustal" magmas ∼200 ka, thus recording the CVZ "baseline" isotopic character of the enriched upper mantle or lower crustal MASH. Thus by ∼200 ka, the buffering feedbacks of upper crustal MASH in the APMB, were no longer a factor. In contrast to "crustal" dacites and andesites being delivered to pre-eruptive chambers during the flare-up, more "parental" basaltic-andesites were able to ascend with only limited modification at ∼20 km, and heterogeneities were maintained in the individual lavas. These changes in the upper crustal magma dynamics at the PCVC can be examined in the context of the regional evolution and thermal state of the CVZ arc from 1 Ma to present.

9. Recording the waning of a flare-up

The changes observed at the PCVC reflect the thermomechanical history of the crust during the waning of the flare-up and return to steady state conditions. As the thermal engine drives a thermal and magmatic front through the crust, feedbacks lead to extensive magmatism in the mid and upper crust (de Silva and Gregg, 2014). As the mantle power input wanes, so does the intensity of upper crustal MASH zone. The evolution of this zone has a profound influence on the upper crust. In the case of the APVC, this crustal magmatic zone is represented by the APMB. A 2-D, conductive heat flow model (de Silva and Gosnold, 2007) illustrates the response of the CVZ crustal geothermal gradients to the development of this zone. After 1 Myr the local geothermal gradient (within ∼2 km of the heat source) would elevate to above the wet solidus of the average CVZ crust. At 5 Myr the geothermal gradient would elevate to where the brittle–ductile transition (BDT) extends into the upper crust. Intrusion of magmas into this thermally prepared upper crustal environment could elevate the local geotherms and BDT to ∼2 km depth depending on emplacement depths of magma bodies.

The high degrees of upper crustal assimilation needed to explain the compositional and isotopic character of the Purico ignimbrite are consistent with upper crustal temperatures exceeding the estimated wet solidus of the regional basement. During the formation of the Purico magmatic system, the crust would have been thermally primed following ∼10 Myr of high mantle heat input. de Silva and Gosnold (2007) estimated intrusive rates on the order of 0.012 and 0.06 $km^3\,yr^{-1}$ during the peak of the flare-up, which are consistent with flux rates estimated for other large silicic magmatic systems (e.g., White et al., 2006). The PCVC developed close to ground-zero for the flare-up which appears to have had its focal point ∼25 km E of the PCVC underneath the Guacha and La Pacana caldera systems. Significant assimilation and melting in the thermally matured upper crust is indicated. Elevated geotherms and associated temperature-dependent effects, such as elevation of the brittle–ductile transition in the uppermost crust would have permitted the accumulation and incubation of the large crystal-rich magma body (e.g., de Silva et al., 2006; Gelman et al., 2013; de Silva and Gregg, 2014) that erupted to deposit the Purico ignimbrite.

In contrast, the lack of evidence for significant modification of lower crustal or mantle derived mafic magmas from Cerro Chascon indicate that the APMB filter (upper crustal MASH) was significantly reduced. The mantle power had dropped to "normal" levels and the thermal engine would have waned by ∼200 ka (Fig. 9). Estimated intrusion rates of 0.00015 to 0.0006 $km^3\,yr^{-1}$ for the steady-state CVZ arc (Francis and Hawkesworth, 1994; de Silva and Gosnold, 2007), similar to rates in other steady-state arc systems (e.g., White et al., 2006; Jicha et al., 2006), are ∼2 to 3 orders of magnitude lower that during the flare up. This decrease would result in a relaxed geotherm and a higher temperature contrast between parental magma and the crust. Ascending "parental" magmas would be emplaced into the shallow crust without being trapped, filtered and processed extensively in the upper crustal MASH zone. The textural, compositional, and isotopic heterogeneity of the Cerro Chascon lavas are also consistent with a decreased geothermal gradient, increased thermal contrast, and relaxation of the brittle–ductile transition from flare-up times. Rather than accommodating large volumes of magma, magmatic addition under colder brittle upper crustal conditions would be more likely to trigger an eruption (Gregg et al., 2012), interrupting any mixing processes and preserving the two distinct magmas.

10. Implications for other continental magmatic arcs

The ignimbrite flare-up in the APVC is recognized as the youngest example of a mature continental arc flare-up sharing many characteristics with the middle Cenozoic volcanic fields of the North American cordillera (e.g. McIntosh et al., 1992; Bryan, 2007; Lipman, 2007; Best et al., 2013). Similar ∼10 to 20 Ma flare-ups events also regularly punctuate the history of long-lived arcs like the Mesozoic Sierra Nevada–Salinia–Mojave arc of the western USA and Mexico (de Silva et al., 2015). If this cyclicity reflects changes in the thermal state of the upper crust in response to changes in the thermal drive from mantle and lower crust (Ducea, 2001; DeCelles et al., 2009), then during flare-ups we would expect that an active upper crustal MASH zone dominates the magma dynamics and this wanes during steady state times. Indeed, the changes in isotopic signatures of magmatism during flare-up and steady state in other areas parallel the changes we have described at the PVCV and in the Central Andes as a whole (e.g., Lipman et al., 1972; Johnson, 1991; Ducea and Barton, 2007), but whether these also manifest at all scales is unknown. Investigations that combine age data with multiscale chemical and isotopic data linked to P–T conditions reveals details of the crustal architecture during different phases of arc evolution, and are a powerful tool for studying fossil arcs.

We emphasize that this model has been developed for mature continental arcs, built on thick crust, in neutral to compressional stress regimes that characterized the active continental margins of the Americas from the Mesozoic through to the present day. Paramount to the operation of the upper crustal MASH zone are the feedbacks between thermal energy, mechanical strength, and magma residence that result during elevated magmatic flux of the flare-up (e.g. de Silva and Gregg, 2014). The model presented in Fig. 10 and its predictions is therefore unlikely to be applicable to arcs in extension where the feedbacks described above are shortcut. For instance, the Taupo Volcanic Zone (TVZ) of New Zealand is often discussed as a modern example of a flare-up, but is recognized for its "hyperactivity" compared to the flare-ups we discuss here. The TVZ lacks the isotopic contrast characteristic of the systems described herein, and has an abundance of basalt interspersed with the silicic eruptions both spatially and temporally (Leonard et al., 2002; Wilson et al., 2006). These differences result from high extension rates and thin, juvenile crust in the TVZ providing pathways for basalt to penetrate silicic reservoirs thus short-cutting the feedbacks that would otherwise promote upper crustal MASH.

11. Conclusions

Our multiscale investigation of the Purico–Chascon Volcanic Complex (PCVC) has revealed that the PCVC preserves a rare temporal sequence of volcanism that records the transition from flare-up to steady-state arc magmatism over an ∼800 kyr period. The transition is recorded at a variety of scales ranging from volcanic landforms to compositional variations within individual crystals. Out of this study we conclude the following:

1) At ∼1 Ma the regional ignimbrite flare-up is recorded in the PCVC. An extensive upper crustal MASH (mixing, assimilation, storage, and homogenization) zone, today evidenced by the low-velocity Altiplano–Puna Magma Body, was processing and supplying andesite and dacite magmas of "crustal" affinity from ∼15 to 20 km to a shallow pre-eruptive reservoir. The 0.98 Ma Purico ignimbrite records the accumulation and eruption of these magmas.

2) Approximately 800 kyr later, the PCVC records a return to steady state arc conditions. Two distinct magmatic environments are recorded in the Chascon dacite lava dome and magmatic inclusions. A shallow (4–8 km) near-solidus crystal mush remnant from the earlier Purico ignimbrite magma is recorded in the Chascon dacite. A second deeper, higher temperature, isotopically parental "baseline" magma derived from the upper mantle/lowermost crust is recorded in the basaltic-andesite inclusions, and inherited plagioclase and amphibole phenocrysts in the Cerro Chascon dacite.

3) The appearance of parental magmas in Cerro Chascon suggests that the vigorous thermal engine associated with the flare-up had relaxed, resulting in the retardation of upper crustal MASH processes, and allowing deeper parental magmas to penetrate to pre-eruptive levels. As these magmas propagate upwards they stage at ∼20 km and re-equilibrate, subsequently rising into the upper crust to interact with and revive remnant crystal-mush.

4) Elevated geotherms and high magmatic fluxes of the flare-up promote homogenization in an extensive upper crustal MASH zone, filtering out the signal of deeper parental magmas. Approximately 800 kyr later, magmatic fluxes 2 to 3 orders of magnitude lower than during the flare-up are implicated. The cooler, brittle conditions in the shallow crust maintain contrast between interacting magmas resulting in the preservation of heterogeneity in steady state eruptions.

5) The PCVC is a microcosm of the Central Andean arc as it transitioned from flare-up to steady state. The imprint of these processes at all scales, from arc, through volcanic landforms, eruptive products to individual crystals, implies that multi-scale investigations, particularly *in situ* isotopes, has significant potential for unraveling large (arc-scale) scale processes.

6) The observations at the PCVC provide a framework to interpret the evolution of magmatic architecture and composition during the flare-ups and steady-state stages in mature continental arcs. Arcs in extension on thin juvenile crust where the feedbacks that promote upper crustal MASH are shortcut are unlikely to conform to this model.

By establishing the relationship between compositional and isotopic signals and distinct pressure–temperature–time pathways for ascending magmas changes during the transition from flare-up to steady-state magmatism we present a method for elucidating the thermal state of a continental magmatic arc by investigating the eruptive products.

Acknowledgements

We would like to thank Arron Steiner, Stephanie Grocke, Jason Kaiser, and Cerise Burns for their comments, which greatly improved this manuscript. The insight and comments of two anonymous journal reviewers and editor Tamsin Mather led to important clarifications and are much appreciated. We would also like to thank Benigno Godoy and Christian Metaluna for enthusiastic help during fieldwork in 2012. We are indebted to the ALMA Observatory for access to private roads and facilities. Adam Kent and the W.M. Keck Collaboratory for plasma spectrometry at OSU and Frank Ramos at New Mexico State University were instrumental in ensuring excellent *in situ* isotopic data. This work was supported by an Oregon State University graduate fellowship, NSF grant EAR 0838536, NSF grant EAR 0908324 that funded the PLUTONS project to which this work contributes, and GSA Graduate Student Research Grant 9767-12.

Appendix A. Supplementary material

Supplementary material related to this article can be found online at http://dx.doi.org/10.1016/j.epsl.2015.04.002.

References

Abot, M., 2009. Development of continental magmatic systems: insights from amphibole chemistry of the Altiplano–Puna Volcanic Complex, central Andes. M.S. thesis. Oregon State University. ScholarsArchive@OSU. http://ir.library.oregonstate.edu/xmlui/handle/1957/12700.

Allmendinger, R.W., Jordan, T.E., Kay, S.M., Isacks, B., 1997. The evolution of the Altiplano–Puna plateau of the Central Andes. Annu. Rev. Earth Planet. Sci. 25, 139–174.

Anderson, J.L., Smith, D.R., 1995. The effects of temperature and f_{O_2} on the Al-in-hornblende barometer. Am. Mineral. 80, 549–559.

Bachmann, O., Bergantz, G.W., 2008. Deciphering magma chamber dynamics from styles of compositional zoning in large silicic ash flow sheets. Rev. Mineral. Geochem. 69, 651–674.

Best, M.G., Christiansen, E.H., Gromme, S., 2013. Introduction: the 36–18 Ma southern Great Basin, USA ignimbrite province and flareup: swarms of subduction-related super volcanoes. Geosphere 9, 260–274. http://dx.doi.org/10.1130/GES00870.1.

Blatter, D.L., Sisson, T.W., Hankins, B., 2013. Crystallization of oxidized, moderately hydrous arc basalt at mid- to lower-crustal pressures: implications for andesite genesis. Contrib. Mineral. Petrol. 166, 861–886.

Bowen, N.L., Tuttle, O.F., 1950. The system $NaAlSi_3O_8$–$KAlSi_3O_8$–H_2O. J. Geol. 58, 489–511.

Bryan, S.E., 2007. Silicic large igneous provinces. Episodes 30, 20–31.

Burns, D.H., 2014. Crustal architecture and magma dynamics in a large continental magmatic system: a case study of the Purico–Chascon volcanic complex, Northern Chile. Ph.D. thesis. Oregon State University. Scholars Archive@OSU. http://hdl.handle.net/1957/50633.

Chmielowski, J., Zandt, G., Haberland, C., 1999. The Central Andean Altiplano–Puna magma body. Geophys. Res. Lett. 26, 783–786.

Coira, B., Davidson, J., Mpodozis, C., Ramos, V., 1982. Tectonic and magmatic evolution of the Andes of Northern Argentina and Chile. Earth-Sci. Rev. 18, 303–332.

Davidson, J.P., de Silva, S.L., Holden, P., Halliday, A.N., 1990. Small-scale disequilibrium in a magmatic inclusion and its more silicic host. J. Geophys. Res. 95, 17,661–17,675.

Davidson, J.P., Harmon, R.S., Worner, G., 1991. The source of central Andean magmas, some considerations. Spec. Pap., Geol. Soc. Am. 265, 233–245.

Davidson, J.P., de Silva, S.L., 1992. Volcanic rocks from the Bolivian Altiplano: insights into crustal structure, contamination, and magma genesis in the central Andes. Geology 20, 1127–1130.

Davidson, J.P., Tepley, F.J., 1997. Recharge in volcanic systems: evidence from isotope profiles of phenocrysts. Science 275, 826–829.

DeCelles, P.G., Ducea, M.N., Kapp, P., Zandt, G., 2009. Cyclicity in Cordilleran orogenic systems. Nat. Geosci. 2, 251–257.

de Silva, S.L., 1989. Altiplano–Puna volcanic complex of the central Andes. Geology 17, 1102–1106.

de Silva, S.L., 1991. Styles of zoning in central Andean ignimbrites, Insights into magma chamber processes. Spec. Pap., Geol. Soc. Am. 265, 217–232.

de Silva, S.L., Francis, P.W., 1991. Volcanoes of the Central Andes. Springer-Verlag, Berlin.

de Silva, S.L., Self, S., Francis, P.W., Drake, R.E., Ramirez, C., 1994. Effusive silicic volcanism in the Central Andes: the Chao dacite and other young lavas of the Altiplano–Puna Volcanic Complex. J. Geophys. Res. 99, 17805–17825.

de Silva, S.L., Zandt, G., Trumbull, R., Viramonte, J.G., Jimenez, G.S.N., 2006. Large ignimbrite eruptions and volcano-tectonic depressions in the Central Andes: a thermomechanical perspective. Geol. Soc. (Lond.) Spec. Publ. 269, 1–17.

de Silva, S.L., Gosnold, W.D., 2007. Episodic construction of batholiths: insights from the spatiotemporal development of an ignimbrite flare-up. J. Volcanol. Geotherm. Res. 167, 320–335.

de Silva, S.L., 2008. Arc magmatism, calderas, and supervolcanoes. Geology 35, 671–672.

de Silva, S.L., Gregg, P.M., 2014. Thermomechanical feedbacks in magmatic systems: implications for growth, longevity, and evolution of large caldera-forming magma reservoirs and their supereruptions. J. Volcanol. Geotherm. Res. 282, 77–91.

de Silva, S.L., Riggs, N.R., Barth, A.P., 2015. Quickening the pulse: fractal tempos in continental arc magmatism. Elements 11, 113–118.

Ducea, M.N., 2001. The California arc: thick granitic batholiths, eclogitic residues, lithospheric-scale thrusting, and magmatic flare-ups. GSA Today 11, 4–10.

Ducea, M.N., Barton, M.D., 2007. Igniting flare-up events in Cordilleran arcs. Geology 35, 1047–1050.

Eichelberger, J.C., 1980. Vesiculation of mafic magma during replenishment of silicic magma reservoirs. Nature 288, 446–450.

Feeley, T.C., Davidson, J.P., 1994. Petrology of calc-alkaline lavas at Volcan Ollague and the origin of compositional diversity at Central Andean Stratovolcanoes. J. Petrol. 35, 1295–1340.

Folkes, C.B., de Silva, S.L., Wright, H.M., Cas, R.A.S., 2011. Geochemical homogeneity of a long-lived, large silicic system, evidence from the Cerro Galán caldera, NW Argentina. Bull. Volcanol. 73, 1455–1486.

Francis, P.W., McDonough, W.F., Hammill, M., O'Callaghan, L.J.O., Thorpe, R.S., 1984. The Cerro Purico shield complex, North Chile. In: Harmon, R.S., Barreiro, B.A. (Eds.), Andean Magmatism, Chemical and Isotopic Constraints. Shiva Publishing, United Kingdom, pp. 106–123.

Francis, P.W., Hawkesworth, C.J., 1994. Late Cenozoic rates of magmatic activity in the Central Andes and their relationships to continental crust formation and thickening. J. Geol. Soc. 151, 845–854.

Gelman, S.E., Gutiérrez, F.J., Bachmann, O., 2013. On the longevity of large upper crustal silicic magma reservoirs. Geology 41, 759–762.

Gregg, P.M., de Silva, S.L., Grosfils, E.B., Parmigiani, J.P., 2012. Catastrophic caldera-forming eruptions: thermomechanics and implications for eruption triggering and maximum caldera dimensions on Earth. J. Volcanol. Geotherm. Res. 241–242, 1–12.

Grunder, A.L., Klemetti, E.W., Feeley, T.C., McKee, C.M., 2008. Eleven million years of arc volcanism at the Aucanquilcha Volcanic Cluster, northern Chilean Andes: implications for the life span and emplacement of plutons. Trans. R. Soc. Edinb. Earth Sci. 97, 415–436.

Hawkesworth, C.J., Hammill, M., Gledhill, A.R., van Calsteren, P., Rogers, G., 1982. Isotope and trace element evidence for late-stage intra-crustal melting in the High Andes. Earth Planet. Sci. Lett. 58, 240–254.

Holland, J.D., Blundy, T.J.B., 1994. Calcic amphibole equilibria and a new amphibole $\pm$ plagioclase geothermometer. Contrib. Mineral. Petrol. 104, 208–224.

Jicha, B.R., Scholl, D.W., Singer, B.S., Yogodzinski, G.M., 2006. Revised age of Aleutian Island Arc formation implies high rate of magma production. Geology 34, 661–664.

Johnson, C.M., 1991. Large-scale crust formation and lithospheric modification beneath middle to late Cenozoic calderas and volcanic fields, western North America. J. Geophys. Res. 96, 13,485–13,507.

Kay, S.M., Coira, B.L., Caffe, P.J., Chen, C.-H., 2010. Regional chemical diversity, crustal and mantle sources and evolution of central Andean Puna plateau ignimbrites. J. Volcanol. Geotherm. Res. 198, 81–111.

Leake, B.E., Woolley, A.R., Arps, C.E.S., Birch, W.D., Gilbert, M.C., Grice, J.D., Hawthorne, F.C., Kato, A., Kisch, H.J., Krivovichev, V.G., Linthout, K., Laird, J., Mandarino, J.A., Maresch, W.V., Nickel, E.H., Rock, N.M.S., Schumacher, J.C., Smith, D.C., Stephenson, N.C.N., Ungaretti, L., Whittaker, E.J.W., Youzhi, G., 1997. Nomenclature of amphiboles: report of the subcommittee on amphiboles of the international mineralogical association, commission of new minerals and mineral names. Can. Mineral. 35, 219–246.

Leonard, G.S., Cole, J.W., Nairn, I.A., Self, S., 2002. Basalt triggering of the c. AD 1305 Kaharoa rhyolite eruption, Tarawera Volcanic Complex, New Zealand. J. Volcanol. Geotherm. Res. 115, 461–486.

Lindsay, J.M., Schmitt, A.K., Trumbull, R.B., de Silva, S.L., Siebel, W., Emmermann, R., 2001. Magmatic evolution of the La Pacana caldera system, central Andes, Chile: compositional variation of two cogenetic, large-volume felsic ignimbrites. J. Petrol. 42, 459–486.

Lipman, P.W., Prostka, H.J., Christiansen, R.L., 1972. Cenozoic volcanism and plate-tectonic evolution of the western United States. I. Early and Middle Cenozoic. Philos. Trans. R. Soc. Lond. A 271, 217–248.

Lipman, P.W., Doe, B.R., Hedge, C.E., Steven, T.A., 1978. Petrologic evolution of the San Juan volcanic field, southwestern Colorado: Pb and Sr isotope evidence. Geol. Soc. Am. Bull. 89, 59–82.

Lipman, P.W., 2007. Incremental assembly and prolonged consolidation of Cordilleran magma chambers: evidence from the Southern Rocky Mountain volcanic field. Geosphere 3, 42–70.

Mamani, M., Worner, G., Sempere, T., 2010. Geochemical variations in igneous rocks of the Central Andean orocline (13°S to 18°S): tracing crustal thickening and magma generation through time and space. Geol. Soc. Am. Bull. 122, 162–182.

McIntosh, W.C., Chapin, C.E., Ratté, J.C., Sutter, J.F., 1992. Time stratigraphic framework for the Eocene–Oligocene Mogollon–Datil volcanic field, southwest New Mexico. Geol. Soc. Am. Bull. 104, 851–871.

Ort, M.H., Coira, B.L., Mazzoni, M.M., 1996. Generation of a crust–mantle magma mixture: magma sources and contamination at Cerro Panizos, Central Andes. Contrib. Mineral. Petrol. 123, 308–322.

Ridolfi, F., Renzulli, A., Puerini, M., 2010. Stability and chemical equilibrium of amphibole in calc-alkaline magmas: an overview, new thermobarometric formulations and application to subduction-related volcanoes. Contrib. Mineral. Petrol. 160, 45–66.

Ridolfi, F., Renzulli, A., 2012. Calcic amphiboles in calc-alkaline and alkaline magmas: thermobarometric and chemometric empirical equations valid up to 1130 °C and 2.2 GPa. Contrib. Mineral. Petrol. 163, 877–895.

Rogers, G., Hawkesworth, C.J., 1989. A geochemical traverse across the North Chilean Andes: evidence for crust generation from the mantle wedge. Earth Planet. Sci. Lett. 91, 271–285.

Salisbury, M.J., Jicha, B.R., de Silva, S.L., Singer, B.S., Jiménez, N.C., Ort, M.H., 2011. $^{40}Ar/^{39}Ar$ chronostratigraphy of Altiplano–Puna volcanic complex ignimbrites reveals the development of a major magmatic province. Geol. Soc. Am. Bull. 123, 821–840.

Schmitt, A., de Silva, S., Trumbull, R., Emmermann, R., 2001. Magma evolution in the Purico ignimbrite complex, northern Chile: evidence for zoning of a dacitic magma by injection of rhyolitic melts following mafic recharge. Contrib. Mineral. Petrol. 140, 680–700.

Tepley, F.J., Davidson, J.P., Clynne, M.A., 1999. Magmatic interactions as recorded in plagioclase phenocrysts of chaos crags, Lassen Volcanic Center, California. J. Petrol. 40, 787–806.

Vernon, R.H., 1986. K-feldspar megacrysts in granites – phenocrysts, not porphyroblasts. Earth-Sci. Rev. 23, 1–63.

Ward, K.M., Zandt, G., Beck, S.L., Christensen, D.H., McFarlin, H., 2014. Seismic imaging of the magmatic underpinnings beneath the Altiplano–Puna volcanic complex from the joint inversion of surface wave dispersion and receiver functions. Earth Planet. Sci. Lett. 404, 43–53.

Watts, R.B., de Silva, S.L., Jimenez de Rios, G., Croudace, I., 1999. Effusive eruption of viscous silicic magma triggered and driven by recharge: a case study of the Cerro Chascon–Runtu Jarita Dome Complex in Southwest Bolivia. Bull. Volcanol. 60, 241–264.

White, S.M., Crisp, J.A., Spera, F.J., 2006. Long-term volumetric eruption rates and magma budgets. Geochem. Geophys. Geosyst. 7, 1–20.

Wilson, C.J., Blake, S., Charlier, B.L.A., Sutton, A.N., 2006. The 26.5 ka Oruanui eruption, Taupo Volcano, New Zealand: development, characteristics and evacuation of a large rhyolitic magma body. J. Petrol. 47, 35–69.